Neurobiology of Disease 121 (2019) 338–349

Contents lists available at ScienceDirect

Neurobiology of Disease

journal homepage: www.elsevier.com/locate/ynbdi

NMDA receptor GluN2D subunit participates to levodopa-induced dyskinesia pathophysiology

Manuela Mellone[a], Elisa Zianni[a], Jennifer Stanic[a,1], Federica Campanelli[b], Gioia Marino[b], Veronica Ghiglieri[b,c], Annalisa Longhi[a], Marie-Laure Thiolat[d,e], Qin Li[f,g], Paolo Calabresi[b,h], Erwan Bezard[d,e,f,g], Barbara Picconi[i], Monica Di Luca[a], Fabrizio Gardoni[a,*]

[a] Dipartimento di Scienze Farmacologiche e Biomolecolari (DiSFeB), Università degli Studi di Milano – La Statale, 20133 Milano, Italy
[b] Laboratory of Neurophysiology, Santa Lucia Foundation, IRCCS, 00100 Rome, Italy
[c] Department of Philosophy, Human, Social and Educational Sciences, University of Perugia, 06100 Perugia, Italy
[d] Université de Bordeaux, Institut des Maladies Neurodégénératives, UMR 5293, F-33000 Bordeaux, France
[e] CNRS, Institut des Maladies Neurodégénératives, UMR 5293, F-33000 Bordeaux, France
[f] Motac Neuroscience Ltd, Manchester, United Kingdom
[g] Institute of Laboratory Animal Sciences, China Academy of Medical Sciences, Beijing, China
[h] Clinica Neurologica, Università degli studi di Perugia, Ospedale Santa Maria della Misericordia, S. Andrea delle Fratte, 06156 Perugia, Italy
[i] Experimental Neurophysiology Laboratory, IRCCS San Raffaele Pisana, University San Raffaele, Rome, Italy

ARTICLE INFO

Keywords:
NMDA receptor
GluN2D
Parkinson's disease
Levodopa-induced dyskinesia
Pharmacological target

ABSTRACT

In the striatum, specific *N*-methyl-D-aspartate receptor (NMDAR) subtypes are found in different neuronal cells. Spiny projection neurons (SPNs) are characterized by NMDARs expressing GluN2A and GluN2B subunits, while GluN2D is exclusively detected in striatal cholinergic interneurons (ChIs). In Parkinson's disease (PD), dopamine depletion and prolonged treatment with levodopa (L-DOPA) trigger adaptive changes in the glutamatergic transmission from the cortex to the striatum, also resulting in the aberrant function of striatal NMDARs. While modifications of GluN2A- and GluN2B-NMDARs in SPNs have been extensively documented, only few studies report GluN2D dysfunction in PD and no data are available in L-DOPA-induced dyskinesia (LID). Here we investigate the contribution of a specific NMDAR subtype (GluN2D-NMDAR) to PD and LID, and whether this receptor could represent a candidate for future pharmacological interventions. Our results show that GluN2D synaptic abundance is selectively augmented in the striatum of L-DOPA-treated male parkinsonian rats displaying a dyskinetic phenotype. This event is associated to a dramatic increase in GluN2D binding to the postsynaptic protein scaffold PSD-95. Moreover, immunohistochemistry and electrophysiology experiments reveal that GluN2D-NMDARs are expressed not only by striatal ChIs but also by SPNs in dyskinetic rats. Notably, in vivo treatment with a well-characterized GluN2D antagonist ameliorates the severity of established dyskinesia in L-DOPA-treated animals. Our findings support a role for GluN2D-NMDARs in LID, and they confirm that cell-type and subunit specific modifications of NMDARs underlie the pathophysiology of LID.

1. Introduction

N-methyl-D-aspartate receptors (NMDARs) are ionotropic glutamate-gated channels which can be classified into different subtypes according to their subunit composition. GluN2D-containing NMDAR is a less prominent but physiologically relevant subtype. Compared to the more abundant GluN2A and GluN2B regulatory subunits, GluN2D confers unique functional properties to NMDARs, such as low sensitivity to Mg^{2+} blockade and slow deactivation time (Glasgow et al., 2015; Monyer et al., 1994; Traynelis et al., 2010; Vicini et al., 1998). At present, little is still known about the functional role of GluN2D in the central nervous system (CNS), even though several studies have indicated that it is expressed in many brain areas and neuronal cell-types. In particular, GluN2D-containing NMDARs are present in the adult rodent brain at different expression levels in the thalamus, subthalamic nuclei, globus pallidus, striatum, substantia nigra, cortex and hippocampus (Bloomfield et al., 2007; Dunah et al., 1998; Perszyk et al., 2016; Swanger et al., 2015; Wenzel et al., 1996; Standaert et al., 1994).

* Corresponding author at: via G. Balzaretti 9, 20133 Milano, Italy.
E-mail address: fabrizio.gardoni@unimi.it (F. Gardoni).
[1] Present address: INSERM, Neurocentre Magendie, Planar Polarity and Plasticity, U1215, Bordeaux, France.

https://doi.org/10.1016/j.nbd.2018.09.021
Received 18 July 2018; Received in revised form 11 September 2018; Accepted 23 September 2018
Available online 24 September 2018
0969-9961/ © 2018 Elsevier Inc. All rights reserved.

In the striatum, GluN2D subunit is localized at the axon terminals of nigrostriatal dopaminergic neurons and in striatal large aspiny cholinergic interneurons (ChIs) (Bloomfield et al., 2007; Jones and Gibb, 2005; Landwehrmeyer et al., 1995; Suárez et al., 2010), where it participates to the crosstalk between dopamine (DA) and glutamate for fine motor control and cognitive functions (Zhang et al., 2014).

The striatum is the main input structure of the basal ganglia, and its activity is the result of a complex integration between different neurotransmitter systems at the two main striatal neuronal populations, namely spiny projection neurons (SPNs) and ChIs (Calabresi et al., 2014). Even if they represent a small portion of striatal cells (≤2%), ChIs play a central role in the physiology of the striatum (Bonsi et al., 2011; Goldberg et al., 2012; Pisani et al., 2007). Indeed, ChIs receive and integrate DAergic and glutamatergic afferents from the *Substantia Nigra pars compacta* (SNpc) and the cortex/thalamus, respectively. This signaling integration results in the stimulation or inhibition of acetylcholine (ACh) release from ChIs. ChI-derived ACh controls SPN excitability both directly through its interaction with postsynaptic M1 and M4 muscarinic receptors expressed on SPNs, and indirectly through the modulation of glutamatergic corticostriatal inputs and local DA release from the nigrostriatal projections (English et al., 2011; Kaneko et al., 2000; Pakhotin and Bracci, 2007; Threlfell et al., 2012). Interestingly, a work by Zhang et al. (2014) demonstrated that GluN2D-NMDARs expressed by ChIs are involved in the inhibition of NMDAR-evoked DA release and of glutamatergic transmission.

The functional interplay between SPNs and ChIs is essential for driving a physiological motor behavior (Calabresi et al., 2007) and SPN/ChI dysfunctional interaction has been reported in several motor disorders, including Parkinson's disease (PD) (Pisani et al., 2007; Tozzi et al., 2016). PD is a common and disabling neurodegenerative disease which is characterized by the progressive loss of DAergic neurons in the SNpc (Goedert et al., 2017). This causes a dramatic reduction in striatal DA content, leading to an imbalance in other neurotransmitter systems of the basal ganglia circuitry. Early studies demonstrated that nigrostriatal pathway degeneration and the following DA depletion lead to significant morphological and functional changes in the glutamatergic signaling from the cortex to the striatum. Augmented presynaptic release of glutamate and aberrant subcellular localization and activity of postsynaptic glutamate receptors have been described in experimental models of PD (Centonze et al., 1999; Gardoni and Di Luca, 2015; Paillé et al., 2010). While changes at the corticostriatal glutamatergic synapse have been extensively studied, less information is available on the modifications of ChI-SPN cross-talk following DA denervation. Few studies reported modifications of ChIs GluN2D-NMDARs in the striatum of a mouse model of PD (Feng et al., 2014; Zhang et al., 2014) and the appearance of GluN2D-NMDARs in SPNs of dopamine-depleted striatum (Zhang and Chergui, 2015).

Levodopa (L-DOPA) remains the major therapeutic approach for PD (Connolly and Lang, 2014), however patients treated for several years and/or with high doses of the drug develop disabling motor complications known as L-DOPA-induced-dyskinesia (LID) (Bastide et al., 2015). The clinical management of these severe side effects is poor, and only the low-affinity noncompetitive NMDAR antagonist amantadine has shown at least a short-term benefit in the treatment of LID without major side effects (Da Silva-Júnior et al., 2005; Elahi et al., 2012; Merello et al., 1999; Moreau et al., 2013; Ory-Magne et al., 2014; Varanese et al., 2010; Wolf et al., 2010). Excessive and aberrant glutamatergic transmission has been reported at the corticostriatal synapse both in animal models and PD patients (Bastide et al., 2015; Mellone and Gardoni, 2018; Picconi et al., 2018). In particular, our work demonstrated the role of altered synaptic GluN2A/GluN2B ratio of NMDARs at the dendritic spine of SPNs (Gardoni et al., 2006, 2012; Mellone et al., 2015). Interestingly, changes in the cholinergic signaling have been documented not only in PD but also in LID (Perez et al., 2018), and preclinical studies focused on the modulation of muscarinic and nicotinic cholinergic receptors as potential therapeutic intervention for LID (Bastide et al., 2015). However, considering the role of ChIs NMDARs in regulating DA release and glutamatergic transmission in the striatal network, we asked whether glutamate receptors expressing GluN2D subunit could play a role in the development of a dyskinetic motor behavior in preclinical models of PD.

2. Materials and methods

2.1. Animals

Adult male Sprague Dawley rats (Charles River Laboratories, Calco, Italy) were housed on a 12-hour (h) light/dark cycle in a temperature-controlled room (20–22 °C) with food and water *ad libitum*. Procedures on rats were carried out according to the European Communities Council Directive 2010/63/EU and the current Italian Law on the welfare of the laboratory animal (D.Lgs. n.26/2014). Procedures were approved by the Italian Ministry of Health (Authorizazion No. 1171/16).

Captive bred female monkeys (*Macaca mulatta*; Xierin, Beijing) were housed in individual cages under controlled conditions of humidity, temperature, and light with food and water ad libitum. Animal care was supervised by veterinarians skilled in healthcare and maintenance. Experiments were carried out in accordance with European Communities Council Directive of 3rd June 2010 (2010/6106/EU) for care of laboratory animals in an Association for Assessment and Accreditation of Laboratory Animal Care–accredited facility. Procedures were approved by the Institute of Laboratory Animal Science ethical committee.

2.2. Reagents

The following unconjugated primary antibodies were used: mouse monoclonal anti-GluN2D (MAB5578, RRID: AB_838227, Merck, Billerica, MA, USA), rabbit anti-β-actin (A5060, RRID: AB_476738; Merck), mouse monoclonal anti-α-tubulin (T9026, RRID: AB_477593, Merck), rabbit polyclonal anti-DOCK3 (AB75911, RRID: AB_1860278, Abcam, Cambridge, UK), anti-NEDD4 (AB14592, RRID: AB_301364, Abcam) monoclonal PSD-95 (75–028, RRID: AB_2307331, Neuromab, Davis, CA, USA), goat polyclonal anti-ChAT (NBP1–30052, RRID: AB_1968484, Novus Biologicals, Littleton, CO, USA), rabbit monoclonal anti-DARPP-32 (2306, RRID: AB_823479, Cell Signaling Technology, Danvers, MA, USA). Alexa Fluor-conjugated secondary antibodies (Thermo Fisher Scientific, Waltham, MA, USA) were used for immunofluorescence studies, whereas horseradish peroxidase (HRP)-conjugated antibodies were used as secondary antibodies for western blot (Bio-Rad, Hercules, CA, USA). Details of the primary antibodies used in the different experimental techniques (co-IP, co-immunoprecipitation; IHC, immunohistochemistry; WB, western blot) are reported below:

Ab Name	Type	Protein MW	Dilution	Application
GluN2D	Mouse	145 kDa	1 µg	co-IP
			1:500	WB
			1:250	IHC
β-ACTIN	Rabbit	42 kDa	1:2000	WB
α-TUBULIN	Mouse	55 kDa	1:10000	WB
DOCK3	Rabbit	233 kDa	1:1000	WB
NEDD4	Rabbit	120 kDa	1:5000	WB
PSD-95	Mouse	95 kDa	1:2000	WB
ChAT	Goat	70 kDa	1:500	IHC
DARPP32	Rabbit	32 kDa	1:1000	IHC

6-hydroxydopamine hydrochloride (6-OHDA; H4381),

apomorphine (A4393), L-DOPA (D1507) and beserazide (B7283) were purchased from Merck. NMDAR GluN2D antagonist UBP141 (ab120193; Abcam) was dissolved in twice an equal molar amount of NaOH solution and diluted in saline for in vivo administration (Lozovava et al., 2014: Morley et al., 2005).

2.3. 6-hydroxydopamine (6-OHDA) rat model of PD

Male rats underwent a stereotaxic injection of 6-OHDA (3 μg/μl, tot. volume of injection: 4 μl, rate of injection: 0.38 μl/min; Sigma-Aldrich) in the left medial forebrain bundle (MFB; coordinates: AP -4.4, ML: +1.2, DV: -7.5) as previously reported (Mellone et al., 2015) to induce degeneration of the nigrostriatal pathway. Fifteen days after the surgery, an apomorphine challenge (0.05 mg/kg, subcutaneous [s.c.] injection) was used to test the success of the nigrostriatal degeneration, and the contralateral turns were counted for 40 min after the injection. The animals performing between 20 and 100 turns were characterized by a partial degeneration of the nigrostriatal pathway (6-OHDA Partial), while those performing at least 200 turns showed > 90% dopaminergic loss were classified as fully-lesioned rats (6-OHDA Full) (Paillé et al., 2010). The severity of the lesion was also confirmed on striatal protein extracts by western blot (WB) with an anti-TH antibody. Ninety days after the apomorphine test, part of 6-OHDA rats with a complete (> 90%) DA depletion (6-OHDA Full) were sacrificed for biochemical and immunohistochemical studies, while the rest of the animals was treated with L-DOPA as described below.

2.4. L-DOPA treatment and abnormal involuntary movements (AIMs) evaluation in the 6-OHDA rat

Fully-lesioned animals were treated with a daily s.c. injection of 6 mg/Kg L-DOPA in combination with 6 mg/Kg benserazide for 14 days (Ghiglieri et al., 2015; Mellone et al., 2015; Stanic et al., 2016; Stanic et al., 2017; Tronci et al., 2014). The onset and severity of L-DOPA-induced dyskinetic behavior was classified according to a highly validated abnormal involuntary movements (AIMs) scale on days 4, 7, 10 and 14 of treatment (Cenci and Lundblad, 2007; Gardoni et al., 2006; Lundblad et al., 2002; Picconi et al., 2003), and animals were divided in dyskinetic and non dyskinetic. Briefly, rats were individually observed for 1 minute (min) every 20 min from 20 to 140 min after L-DOPA administration. At each observation time point, 3 subtypes of AIMs were evaluated: i. axial (dystonic or choreiform torsion of the upper part of the body towards the side contralateral to the lesion), ii. limb (jerky and/or dystonic movements of the forelimb contralateral to the lesion) and iii. orolingual (empty jaw movements and tongue protrusion). Each of these subtypes was scored on a severity scale from 0 to 4: 0 = absent, 1 = present during less than half of the observation time (≤ 30 sec), 2 = present for more than half of the observation time (> 30 sec), 3 = present all the time (= 1 min) but suppressible by an external stimulus, and 4 = present all the time and not suppressible by an external stimulus. The total AIMs score for each test session (4, 7, 10, 14 days) was obtained by summing the scores of the 3 AIMs subtypes (axial, limb, orolingual) at all observation time points (from 20 to 140 min after L-DOPA injection).

For the molecular and immunohistochemical studies, dyskinetic and non dyskinetic rats were sacrificed 1 h after the last daily L-DOPA injection at L-DOPA peak dose (Gardoni et al., 2006). NMDAR GluN2D antagonist UBP141 was administrated to dyskinetic animals with a single intraperitoneal (i.p.) or intrastriatal (i.s.) injection. For the latter, dyskinetic rats underwent a single stereotaxic injection of 5 nmol UBP141/saline in the ipsilateral striatum (rate of injection 0.5 μl/min; AP: +0.2, L: +3.5, DV: −5.7) on day 15 of L-DOPA treatment. To evaluate the effect of UBP141 on LID, behavioral assessments (AIMs) were carried out in a double-blinded fashion the day before the surgery/i.p. injection (−18 h before UBP141 i.s. injection or day −1, respectively) and on the day of the surgery/i.p. injection (6 h after UBP141 i.s. or day 0, respectively).

2.5. 1-Methyl-4-Phenyl-1,2,3,6-Tetrahydropyridine (MPTP) monkey model of PD and L-DOPA-induced dyskinesia

Disease modelling in non-human primates and tissue collection took advantage of a previously used and described experimental cohort (Bourdenx et al., 2015; Santini et al., 2010; Stanic et al., 2017). MPTP intoxication protocol, chronic L-DOPA treatment, clinical assessments, terminal procedure and the characterization of the extent of nigrostriatal denervation were conducted as previously published (Ahmed et al., 2010; Porras et al., 2012; Santini et al., 2010; Urs et al., 2015). Briefly, macaques received daily saline or MPTP hydrochloride injections (0.2 mg/kg, intravenously) until parkinsonian signs appeared. Once PD motor signs were stable, MPTP-treated monkeys were either untreated or treated twice a day with individually titrated dose of L-DOPA (Madopar, L-DOPA/carbidopa, 4:1 ratio; range, 9–17 mg/kg). This dose, defined as 100% dose, was used for chronic L-DOPA treatment, which lasted for 4 to 5 months until dyskinesia stabilized. DAT binding autoradiography with [125I]-(*E*)-N-(3-iodoprop-2-enyl)-2ßcarboxymethyl-3ß-(4′-methylphenyl)-nortropane (Chelatec, France) showed a dramatic and similar reduction (N95%) in all MPTP-treated groups in comparison to control animals (data not shown), as previously described (Fernagut et al., 2010). Brain patches collected from 300 μm-thick fresh frozen coronal sections containing caudate-putamen were collected for WB analysis.

2.6. Subcellular fractionation for postsynaptic proteins

This method allows for the purification of highly-enriched postsynaptic proteins from a tissue preparation (Gardoni et al., 2006) with the absence of presynaptic markers. The ipsilateral and contralateral striata from 6-OHDA rats with a partial or complete nigrostriatal lesion (6-OHDA Partial and Full, respectively), and the ipsilateral striatum from dyskinetic (Dys) and non dyskinetic (Non Dys) rats were homogenized with a hand-held Teflon-glass potter at 4 °C in ice-cold buffer (pH 7.4) containing 0.32 M sucrose, 1 mM Hepes, 1 mM $MgCl_2$, 1 mM $NaHCO_3$ and 0.1 phenylmethanesulfonylfluoride supplemented with protease (Complete™ Cocktail, Merck) and phosphatase (PhosSTOP™, Merck) inhibitors. An aliquot of the homogenate was frozen at −20 °C, while the rest of the sample was centrifugated at 800 g for 5 min at 4 °C to remove nuclear contamination and white matter. The supernatant was collected and spun at 13,000 *g* for 15 min at 4 °C. The resulting pellet (P2 crude membrane fraction) was resuspended in 1 mM Hepes hypotonic buffer supplemented with Complete™ Cocktail. An aliquot of the P2 fraction was stored at −20 °C for co-immunoprecipitation experiments and the remaining part was further centrifugated at 100,000 g for 1 h at 4 °C. Triton X-100 and KCl were added to the sample to a final concentration of 1% and 150 mM, respectively. After a 15-min incubation on ice, the sample was finally spun at 100,000 *g* for 1 h at 4 °C and the final pellet (Triton-insoluble fraction, TIF) was homogenized in a glass-glass homogenizer in 20 mM Hepes supplemented with Complete™ tablets and finally stored at −20 °C until use.

TIF purification from striatal patches of control, parkinsonian MPTP-treated and dyskinetic MPTP monkey was performed with a shortened protocol due to the limited amount of starting material (5 mg tissue/animal). Striatal patches from the different experimental groups were homogenized with a glass-glass potter in 300 μl of the same ice-cold lysis buffer. A small portion of the homogenate was collected and stored at −20 °C, while the rest of the sample was centrifugated at 13.000*g*× 15 min at 4°C. The resulting pellet was immediately resuspended in 300 μl of 0.5% Triton and 150 mM KCl supplemented with Complete™ Tablets and incubated on ice for 15 min before centrifugation at 100,000*g* for 1 h at 4 °C. The pellet (TIF) was finally resuspended in 20 mM Hepes and Complete™ in a glass-glass homogenizer. TIF was stored at −20 °C. Similar TIF yields were obtained from the whole

striata or striatal patches of all experimental groups.

2.7. Co-imunoprecipitation (Co-IP)

P2 crude membrane fraction (50 μg) from the ipsilateral and contralateral striata of 6-OHDA Full rats and the ipsilateral striatum of dyskinetic animals were incubated in RIA buffer (200 mM NaCl, 10 mM EDTA, 10 mM Na_2HPO_4, 0.5% Nonidet P-40) and 0.1% sodium dodecyl sulfate (SDS) with an antibody against GluN2D subunit (1 μg) overnight at 4 °C on a wheel. No IgG samples were used as the negative control and were prepared with the same protocol but in absence of the primary antibody. Protein A/G-agarose beads (Santa Cruz Biotechnology, Dallas, TX, USA) were added and incubation was continued for 2 h at room temperature (RT) on the wheel. Beads were collected by gravity and washed in RIA buffer with 0.1% SDS 4 times. Laemmli sample buffer was added to the immunoprecipitates and the mixture was incubated at 100 °C for 10 min. Beads were collected by centrifugation and the supernatant was loaded onto an acrylamide/bisacrylamide gel for SDS-PAGE.

2.8. Western Blot (WB)

Homogenates, TIF or P2 coimmunoprecipitates from rat or monkey tissue were separated onto 7–9% acrylamide/bisacrylamide gels. The percentage was decided in each experiment taking into account the molecular weight of the target proteins. Protein separation was performed with constant current (20–30 mA) in running buffer (10×: 25 mM Trizma base, 1.92 M glycine, 0.1% SDS, pH 8.3/8.6). Proteins were then transferred onto a nitrocellulose membrane (Bio-rad) in blotting buffer (0.192 M glycine, 0.025 M Tris, 20% methanol; pH 8.3). In order to avoid over-heating, the apparatus was kept in wet ice during the transfer. The nitrocellulose membrane was blocked in I-Block solution (Applied Biosystems, Monza, Italy) for 1 h at RT and then incubated with the appropriate primary antibody in I-Block overnight at 4 °C or 3 h at RT. After 3 washes in 0.05% Tween-20 in TBS (TBS-T) for 10–15 min, 3 times and the membrane was HRP-conjugated secondary antibody in I-Block for 1 h at RT. After 3 washes (10–15 min each) in TBS-T, the membrane was developed with Clarity™ Western ECL substrate reagent (Bio-rad). Acquisition and quantification of all images were performed by using ChemiDoc™ MP System (Bio-rad) and Image Lab software (Bio-rad). Also, this software was always applied for the evaluation of the correct molecular weight of all bands before any quantification was performed.

2.9. Free-floating immunohistochemistry (IHC)

Control, fully-lesioned 6-OHDA and dyskinetic rats were perfused with 4% paraformaldehyde (PFA) in 0.1 M phosphate buffered saline (PBS). The brain was removed from the skull and post-fixed in 4% PFA in PBS for 2 h at 4 °C.

For immunofluorescence studies, the brain was sliced in 50 μm coronal sections using the Vibratome 1000 Plus Sectioning System (3 M). Brain slices were incubated in 0.3% Triton X-100 in PBS (0.3% T-PBS) supplemented with 10% normal goat/donkey serum (NGS/NDS) for 1 h at RT, shaking. After permeabilization and blocking, slices were incubated with anti-GluN2D and anti-ChAT or anti-GluN2D and anti-DARPP32 antibodies in 0.1% T-PBS supplemented with 3% NGS/NDS for 3 o/n at 4 °C, shaking. The appropriate Alexa Fluor-conjugated secondary antibodies in 0.1% T-PBS with 3% NGS/NDS were applied for 2 h at RT followed by nuclei staining with the fluorescent dye 4′,6-diamidino-2-phenylindole (DAPI; 1:50,000 in PBS; Thermo Fisher Scientific). Labelling in the ipsilateral striatum was visualized with LSM510 Meta system confocal microscope and AIM 4.2 software (Zeiss, Oberkochen, Germany).

2.10. Electrophysiology

For electrophysiological studies corticostriatal coronal slices were cut from $n = 8$ male rats brains (thickness, 240 μm) using a vibratome (Leica) and stored for 45 min in Krebs' solution containing (in mM): 126 NaCl, 2.5 KCl, 1.2 MgCl2, 1.2 NaH2PO4, 2.4 CaCl2, 10 glucose and 25 NaHCO3, bubbled with a 95% O2 – 5% CO2 gas mixture, to allow recovery. A single slice was then transferred to a recording chamber and submerged in continuously flowing Krebs' solution (RT; 2.5–3 ml/min). Whole-cell patch-clamp recordings were performed on SPNs and ChIs, visualized using infrared differential interference contrast microscopy in the dorsal striatum (Eclipse FN1, Nikon). Recordings were made with a Multiclamp 700B amplifier (Molecular Devices), using borosilicate glass pipettes (outer diameter, 1.5 mm; inner diameter, 0.86 mm) pulled on a P-1000 Puller (Sutter Instruments). Pipette resistances ranged from 3.5 to 6 MΩ. The internal solution for patch-clamp recordings NMDA receptor-mediated currents contained (in mM): 120 CsMeSO3, 10 CsCl, 8 NaCl, 2 MgCl2, 10 HEPES, 0.2 EGTA, 10 TEA, 5 QX314, 0.3 NaGTP and 2 Mg-ATP. The compounds were dissolved in NaOH solution and aliquoted. Drugs were applied by dissolving them to the desired final concentration in the external Kreb's solution, and bath-applied by switching the Kreb's solution to one containing known concentrations of the drugs. Neurons were held at +40 mV holding membrane potential: SPNs were identified by their hyperpolarized resting membrane potential (RMP, ~ −80 mV), absence of spontaneous action potential discharge. ChIs were localized under IR-DIC visualization by their large soma and subsequently identified by relatively depolarized resting membrane potential (RMP of approximately −60 mV), and long-lasting action potential. The stimulating bipolar electrode was located in the white matter between the cortex and the striatum to activate corticostriatal fibers and evoke excitatory post-synaptic currents (EPSCs). The recording electrodes were placed within the dorsolateral striatum.

Signals were acquired using Axon Digidata 1550 (Axon Instruments), recorded and stored on PC using pClamp 10.5 (Molecular Devices). EPSCs were always recorded in the continuous presence of 50 μM Picrotoxin (Sigma-Aldrich) to block $GABA_A$ receptors if not differently specified. Input resistances and injected currents were monitored throughout the experiments. Variations of these parameters (> 20%) lead to the rejection of the experiment. Quantitative data are expressed as a percentage of EPSC amplitudes compared to the relative control values, the latter representing the mean of responses recorded during a stable period (10–15 min).

2.11. Statistical analysis

Data were analyzed using GraphPad Prism 6.0 (GraphPad Software, La Jolla, CA, USA). Data followed a normal distribution and the significance of the differences was analyzed by unpaired or paired two-tailed Student's *t*-test, one-way or two-way ANOVA followed by Bonferroni or Tukey's post-hoc tests. Data are presented as mean ± SEM and p values are given in the Results section and/or in the Figure legends. Off-line electrophysiological analysis was performed using Clampfit 10.6 (Molecular Devices) and GraphPad Prism 6.0 software. Two-way ANOVA or Student's t-test were established to be appropriate on the basis of variance similarities between groups and normal distribution of the data. Values given in the figures and text are mean ± SE; the number of recorded neurons (n) is provided for each set of experiments. For all experiments, the significance levels were established at $p < .05$ (*), $p < .01$ (**), and $p < .001$ (***). No pooling of tissue from multiple animals has been performed. Accordingly, each experimental sample used in WB and co-IP assays corresponds to the striatum of one animal. A priori power analysis was performed based on previous experience in all experimental approaches used here (Gardoni et al., 2006; Mellone et al., 2015; Tozzi et al., 2016; Stanic et al., 2017) and verified with softwares (i.e. GPower) for power

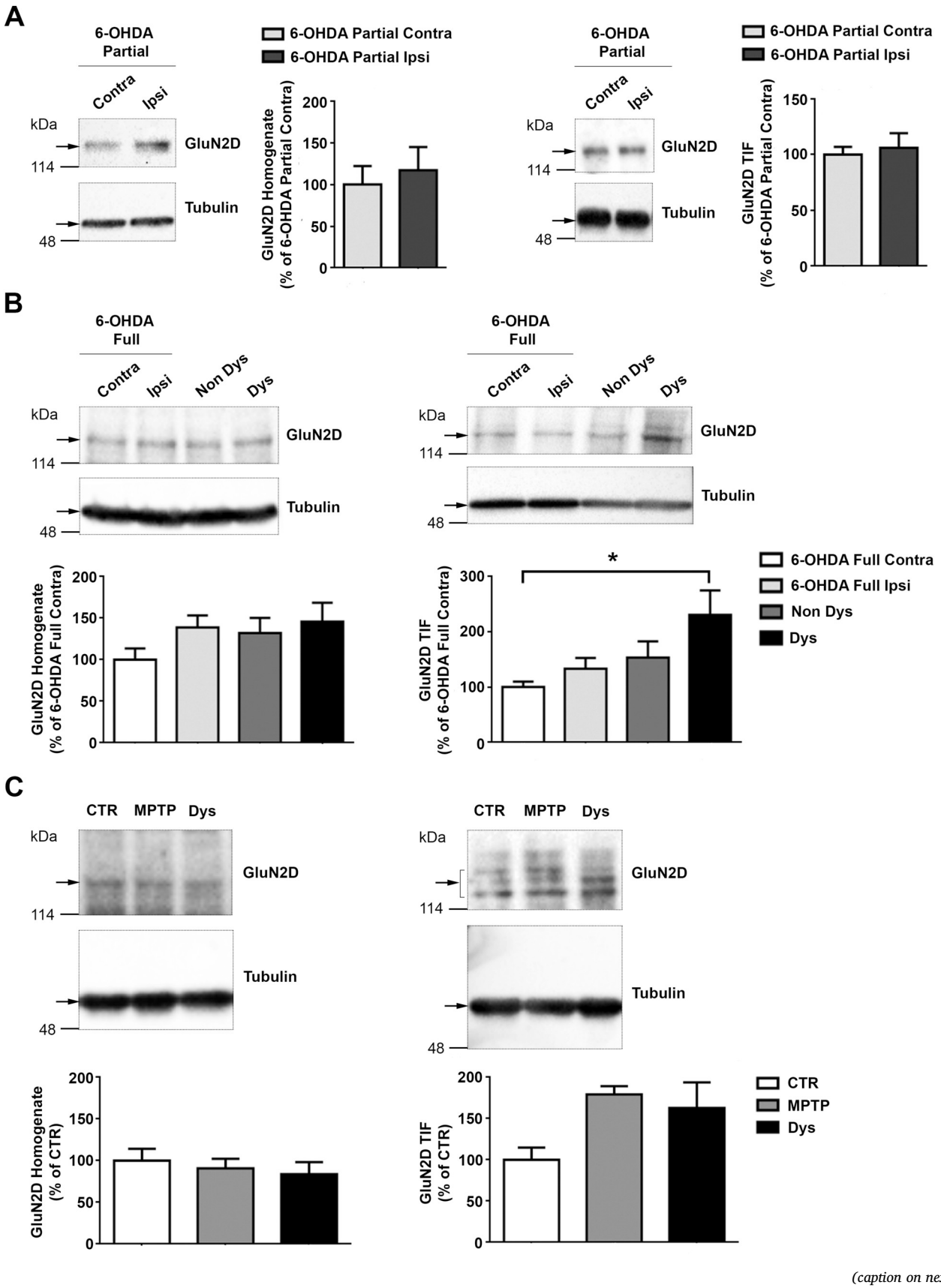

(caption on next page)

Fig. 1. GluN2D-containing NMDARs expression and synaptic distribution in experimental models of PD and LID. WB analysis for GluN2D subunit in the homogenate (left panel) and TIF (right panel) (A) from the ipsilateral and contralateral striata of 6-OHDA-injected rats with a partial lesion of the DAergic pathway (6-OHDA Partial Ipsi and Contra, respectively) - $n = 8$, $p > .05$, unpaired Student's *t*-test; (B) from the ipsilateral and contralateral striata of naïve 6-OHDA-injected rats with a full DA denervation (6-OHDA Full Ipsi and Contra, respectively) and in the ipsilateral striatum of non dyskinetic (Non Dys) and dyskinetic (Dys) animals - one-way ANOVA followed by Tukey's post-hoc test, $n = 9$, $^{*}p < .05$ 6-OHDA Full Contra vs Dys; (C) from striatal patches of control (CTR), MPTP-injected (MPTP) and dyskinetic (Dys) monkeys - $n = 4$, $p = .0534$, one-way ANOVA followed by Tukey's post-hoc test. Data are expressed as % of controls and presented as mean ± SEM. The same amount of proteins was loaded per lane. Histograms show the quantification of WB expressed as percentage of Contra or CTR after normalization on tubulin levels. Tubulin was revealed without the use of any stripping and reprobing procedure onto the same membrane where GluN2D was visualized.

analysis.

3. Results

3.1. NMDAR GluN2D subunit is augmented in experimental models of dyskinesia

We first investigated whether GluN2D-containing NMDARs participate to the adaptive changes occurring in experimental parkinsonism, and whether GluN2D could represent a possible novel target for PD and LID. To do so, we took advantage of a well-validated toxin-based model of PD, namely the 6-OHDA rat. 6-OHDA-injected animals give the possibility to model different levels of DAergic degeneration and subsequent DA depletion (Paillé et al., 2010). Importantly, these animals are routinely used for chronic administration of L-DOPA as a model of experimental LID (Cenci and Lundblad, 2007). First, we questioned whether GluN2D striatal expression and synaptic localization were altered in the disease. Striata from 6-OHDA-injected rats carrying a partial (approximately 75%) or complete lesion of the nigrostriatal pathway (Paillé et al., 2010) were purified to obtain the homogenate and the postsynaptic Triton-insoluble fraction (TIF) for WB analysis (Fig.1A and Fig.1B). No differences in both GluN2D expression (*left panel*, Fig.1A and Fig.1B) and synaptic levels (*right panel*, Fig.1A and Fig.1B) were detected in 6-OHDA rats with a partial (6-OHDA Partial) or complete (6-OHDA Full) lesion of the nigrostriatal pathway (Fig.1A: $n = 8$, $p > .05$, unpaired Student's t-test; Fig.1B: $n = 9$, $p > .05$, one-way ANOVA followed by Tukey's post-hoc analysis). We then evaluated whether chronic L-DOPA administration could affect GluN2D subunit of the NMDAR. While no modifications in GluN2D expression were observed by WB in the total tissue lysate from striata of all experimental groups (*left panel*, Fig.1B), GluN2D levels were significantly increased in the postsynaptic fraction from L-DOPA-treated dyskinetic animals (Dys) (*right panel*, Fig.1B; n = 9, one-way ANOVA: $p = .0178$, Tukey's post-hoc adjustment: $^{*}p < .05$ 6-OHDA Full Contra vs Dys). Notably, no alterations of GluN2D synaptic localization were observed in animals that did not show a dyskinetic profile after L-DOPA treatment (*right panel*, Fig.1B; n = 9, one-way ANOVA: p = .0178, Tukey's post-hoc adjustment: $p > .05$ Non Dys vs 6-OHDA Full Contra).

To support the results obtained in the rat, striatal patches were obtained from control, MPTP-treated parkinsonian and MPTP-treated dyskinetic monkeys. Considering the limited amount of starting material, a shortened version of the synaptic purification protocol was used as indicated in the Materials and Methods section. WB analysis in tissue from non-human primates confirmed that GluN2D expression was unaltered also in this experimental model (*left panel*, Fig.1C; $n = 4$, $p > .05$, one-way ANOVA followed by Tukey's post-hoc test). However, even if a trend towards an augmented level of GluN2D at striatal synapses was observed both in parkinsonian and dyskinetic monkeys, we failed to recapitulate the synaptic changes found in the dyskinetic rats (*right panel*, Fig.1C; n = 4, $p = .0534$, one-way ANOVA followed by Tukey's post-hoc test).

3.2. Association with the scaffolding protein PSD-95 retains GluN2D-NMDARs at the striatal synapses of L-DOPA-treated dyskinetic rats

The increase in the synaptic abundance of GluN2D-containing NMDARs in L-DOPA-treated dyskinetic animals may be associated to different mechanisms, including pathological modifications in the degradation or endocytosis/surface retention of this glutamate receptor (Paoletti et al., 2013). Accordingly, we tested both hypotheses. The E3 ubiquitin ligase neuronally-expressed developmentally downregulated gene 4 (Nedd4), a member of the ubiquitin proteosome system, has been shown to play a role in α-synuclein-induced toxicity in PD (Davies et al., 2014; Rotin and Kumar, 2009; Tofaris et al., 2011). Interestingly, it has been shown that GluN2D subunit is a target of Nedd4 (Gautam et al., 2013), suggesting a new putative mechanism involved in ubiquitin-dependent degradation of GluN2D-containing receptor. To support this hypothesis, we performed WB analysis to detect any difference in Nedd4 levels in the homogenate (*left panel*) and synaptic fraction (TIF, *right panel*) from the contralateral and the ipsilateral striata of parkinsonian rats (6-OHDA Full Contra and Ipsi, respectively) and the ipsilateral striatum of dyskinetic (Dys) animals. No changes in Nedd4 expression nor synaptic distribution were found (Fig.2A; $n = 10$; $p > .05$, one-way ANOVA followed by Tukey's test).

Dedicator of cytokinesis 3 (Dock3), a guanine nucleotide exchange factor, interacts with GluN2D and such binding reduces the surface expression of this NMDAR subtype (Bai et al., 2013). Therefore, Dock3 protein levels were evaluated in the homogenate (*left panel*) and synaptic fraction (*right panel*) from the ipsilateral striatum of parkinsonian rats naïve to L-DOPA (6-OHDA Full Ipsi) and of dyskinetic (Dys) animals (Fig.2B). The contralateral striatum (6-OHDA Full Contra) from parkinsonian rats was used as control. While Dock3 expression did not change in the 3 experimental groups (*left panel*, Fig.2B; $n = 11$ for 6-OHDA Full Contra and Ipsi, n = 10 for Dys; $p > .05$, one-way ANOVA followed by Tukey's post-hoc test), the surface levels of this protein tend to decrease (18%) in the parkinsonian animals displaying a dyskinetic behavior (*right panel*, Fig.2B; n = 11 for 6-OHDA Full Contra and Ipsi, n = 10 for Dys; $p > .05$, one-way ANOVA followed by Tukey's post-hoc test). Similar results were obtained when we analyzed Dock3/GluN2D complex in the P2 crude membrane fraction from naïve and dyskinetic parkinsonian rats (Fig.2C; $n = 5$; $p > .05$, one-way ANOVA followed by Tukey's post-hoc adjustment; 23% reduction Dock3/GluN2D binding in Dys rats compared to 6-OHDA Full Contra).

It is well established that members of the MAGUK family such as the scaffold PSD-95 are involved in the anchoring of NMDAR complexes at the postsynaptic density (Chen et al., 2015; Cousins et al., 2008; Tozzi et al., 2016). An aberrant binding of PSD-95 to both NMDAR GluN2A subunit (Gardoni et al., 2012) and to D1-type DA receptors (Porras et al., 2012) has been previously described in LID. Based on these considerations, we questioned whether GluN2D synaptic levels were augmented due to its increased interaction with PSD-95. P2 crude membrane fractions from the ipsilateral (6-OHDA Full Ipsi) and the contralateral (6-OHDA Full Contra) striata of parkinsonian rats and the ipsilateral striatum of dyskinetic animals (Dys) were immunoprecipitated with an anti-GluN2D antibody and PSD-95 was revealed in the immunocomplexes (Fig.2D). Our results indicated that PSD-95/GluN2D association is significantly augmented in Dys rats (Fig.2D; $n = 7$ for 6-OHDA Full Contra and Ipsi, $n = 6$ for Dys; one-way ANOVA: $p = .0066$, Tukey's post-hoc analysis: $^{**}p < .01$ 6-OHDA Full Contra vs Dys, $^{*}p < .05$ 6-OHDA Full Ipsi vs Dys), suggesting that this NMDAR subtype is retained at the postsynaptic membrane in the striatum of animals displaying a dyskinetic motor behaviour.

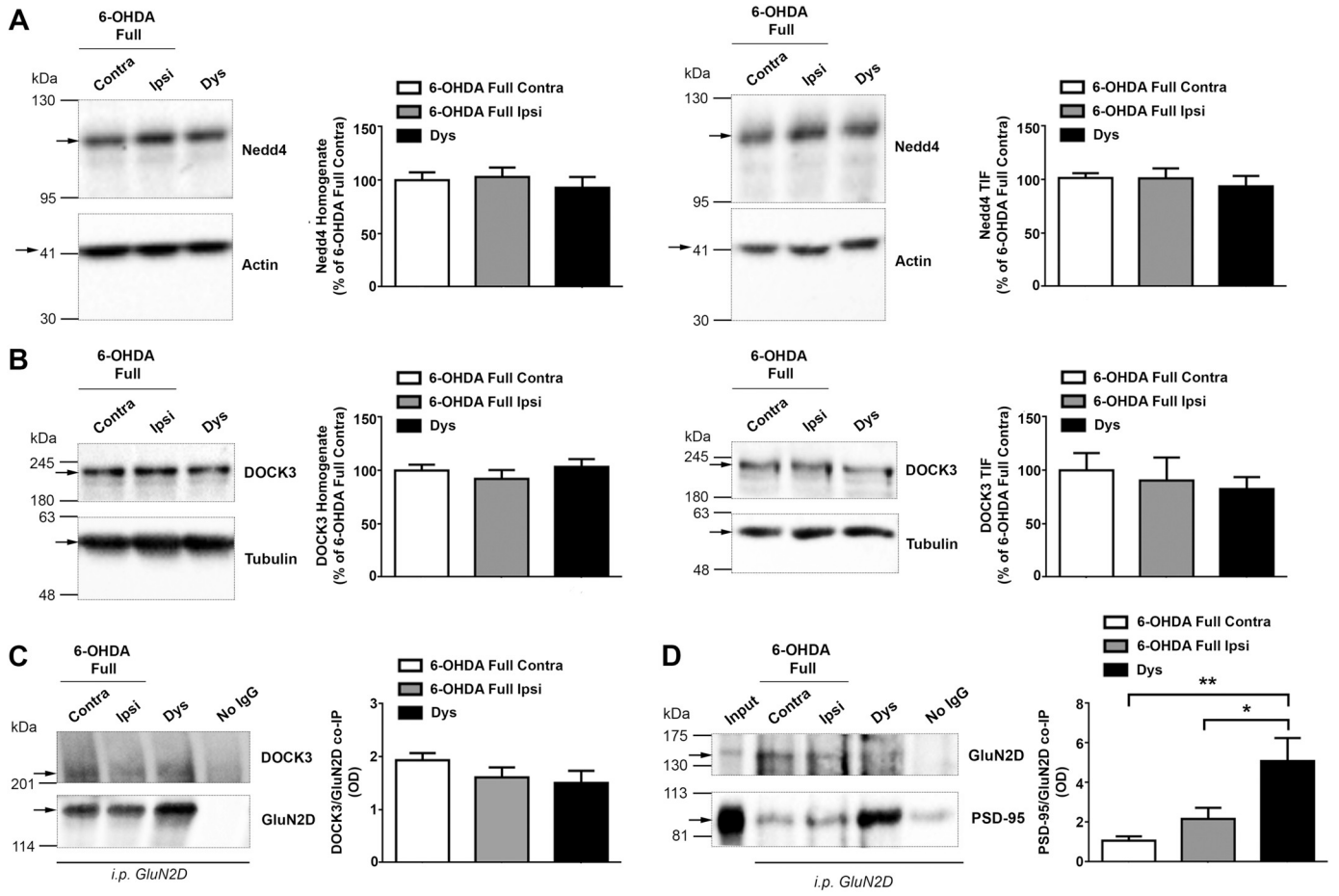

Fig. 2. Study of the association of GluN2D-expressing NMDARs with Nedd4, DOCK3 and PSD-95 in the striatum. (A) WB evaluation of Nedd4 in the homogenate and TIF of 6-OHDA rats with a full degeneration of the nigrostriatal pathway (6-OHDA Full Contra and Ipsi) and of dyskinetic animals (Dys) – $n = 10$, $p \geq .05$, one-way ANOVA followed by Tukey's post-hoc test. (B) DOCK3 expression and synaptic distribution in the ipsilateral striata of parkinsonian (6-OHDA Full Ipsi) and dyskinetic (Dys) rats. The contralateral striatum of naïve 6-OHDA was used as control (6-OHDA Full Contra) - n = 10–11, $p \geq .05$, one-way ANOVA followed by Tukey's adjustment. (A, B) Each lane was loaded with the same amount of proteins. Histograms show the quantification of WB expressed as percentage of 6-OHDA Full Contra after normalization on actin (A) or tubulin (B) levels. Actin (A) and tubulin (B) were detected onto the same membrane used to reveal Nedd4 (A) and DOCK3 (B) respectively without any stripping/reprobing procedure. (C) Co-IP analysis for DOCK3/GluN2D association in P2 crude membrane fraction from 6-OHDA Full Contra, 6-OHDA Full Ipsi and Dys - $n = 5$, $p \geq .05$, one-way ANOVA with Tukey's post-hoc test. DOCK3 band was normalized on the corresponding GluN2D immunoprecipitated band from the same lane. (D) Co-IP for GluN2D and PSD-95 in P2 fraction from the ipsilateral and the contralateral striata of 6-OHDA-lesioned rats (6-OHDA Full Contra and Ipsi, respectively) and the ipsilateral striatum of L-DOPA-treated dyskinetic animals (Dys) - one-way ANOVA followed by Tukey's post-hoc analysis, $n = 6–7$, $^{**}p \leq .01$ 6-OHDA Full Contra vs Dys, $^{*}p \leq .05$ 6-OHDA Full Ipsi vs Dys. 10 µg of the P2 protein sample (20% of the amount of sample used in the co-IP assay) was loaded in the input lane. PSD-95 band was normalized on the corresponding GluN2D immunoprecipitated band from the same lane. Data in (C) and (D) are expressed as optic density (OD). In all four panels results are presented as mean ± SEM.

3.3. GluN2D-NMDARs appear in striatal spiny projection neurons of dyskinetic animals

GluN2D-containing NMDARs are selectively expressed in striatal ChIs (Bloomfield et al., 2007; Tozzi et al., 2016). In agreement with these previous reports, IHC analysis on coronal striatal slices from control rats showed the presence of GluN2D immunoreactivity only in ChAT-positive interneurons (*upper panels*, Fig.3A) and no signal was detected in DARPP32-positive SPNs (*upper panels*, Fig.3B). On the contrary, IHC analysis performed on slices from parkinsonian (6-OHDA Full) and dyskinetic (Dys) rats indicated that GluN2D subunit was also present in striatal SPNs. Importantly, a more intense GluN2D staining in SPNs was observed in tissue from dyskinetic rats compared to 6-OHDA Full striatum (Fig.3A,B).

In agreement with the above-described IHC results, a recent electrophysiological study (Zhang et al., 2015) found that GluN2D is absent at glutamatergic synapses onto SPNs in control striatum, but contributes to NMDAR excitatory postsynaptic currents (EPSCs) in SPNs of the dopamine-depleted striatum. To further confirm our IHC results and to address with a quantitative approach the presence of GluN2D also in SPNs of levodopa-treated dyskinetic rats, striatal EPSCs were recorded in slices of control and dyskinetic 6-OHDA-injected rats. Currents were recorded in control slices and slices exposed to (2*R**,3*S**)-1-(Phenanthrenyl-3-carbonyl)piperazine-2,3-dicarboxylic acid (also known as UBP141) (Costa et al., 2009; Lozovava et al., 2014; Yamamoto et al., 2013), a competitive GluN2D selective antagonist. After acquiring a stable baseline for 10 min, 3 µM UBP141 was applied for further 15 min. As expected, EPSC amplitude was significantly reduced in control ChIs, suggesting an inhibition of glutamatergic postsynaptic evoked transmission in the striatum and, therefore, the selective presence of GluN2D in these interneurons (Fig.4A,C). Conversely, in SPNs, exposure of the slices to 3 µM UBP141 did not change the EPSC amplitude, advancing the absence of GluN2D-containing NMDARs in these neurons in control rats (Fig.4A,B). In fact, in these neurons, 15 min of UBP141 application produced similar EPSC amplitude to that obtained in the absence of the drug (Fig.4B). To explore the expression of GluN2D-containing NMDARs in dyskinetic rats, we exposed corticostriatal slices to 3 µM of the GluN2D inhibitor. Application of UBP141 for 15 min significantly

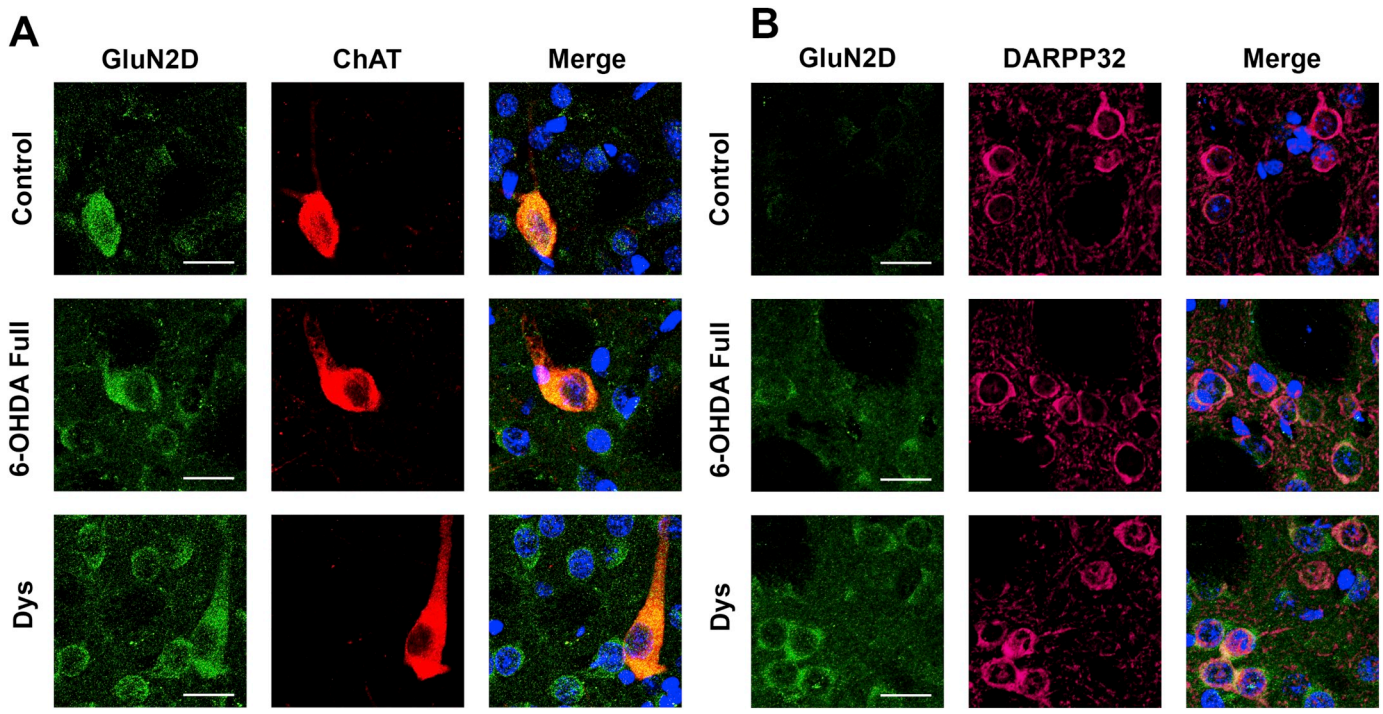

Fig. 3. Immunofluorescence labeling of GluN2D-containing NMDAR expression in the striatum of parkinsonian and dyskinetic animals. Immunohistochemistry on 50 µm-thick coronal slices from the ipsilateral striatum of control, naïve 6-OHDA with a complete DA denervation (6-OHDA Full) and after L-DOPA administration (Dys). (A) Labeling for GluN2D subunit (green) and ChAT (red, ChI marker), and (B) for GluN2D subunit (green) and DARPP32 (pink, SPN marker). Nuclei were stained with DAPI (blue). Scale bar: 25 µm.

reduced the NMDA-mediated EPSC amplitude, similarly to what was observed in ChIs from slices of control rats (Fig.4D,E). In agreement with IHC data, in SPNs of control rats exposure of the slices to UBP141 did not reduced the glutamatergic transmission.

3.4. In vivo modulation of GluN2D-NMDARs ameliorates the dyskinetic motor phenotype of L-DOPA-treated parkinsonian rats

To further support the involvement of GluN2D-containing NMDARs in LID, parkisonian rats chronically treated with L-DOPA and displaying a dyskinetic profile were treated with UBP141. A single stereotaxic injection of 5 nmol UBP141 ($n = 6$) was carried out in the ipsilateral striatum of L-DOPA-treated dyskinetic animals, and the abnormal involuntary movements (AIMs) were scored before (−18 h) and after (6 h) the surgery (Fig.5A). GluN2D inhibition was able to reduce the severity of established dyskinesia 6 h post-surgery (*top panel*, Fig.5A; n = 6; $p = .0007$, paired Student's *t*-test). Moreover, UBP141 also delayed AIMs induction in the treated animals (*lower panel*, Fig.5A; n = 6; 20–60–80-100-120-140 min: $p > .05$-18 h vs 6 h, 40 min: $p = .0117$–18 h vs 6 h, paired Student's t-test). To evaluate the systemic efficacy of GluN2D inhibition, UBP141 was administrated as a single i.p. injection 30 min before the last L-DOPA dose in animals with an established dyskinetic profile. To determine the best experimental conditions for systemic administration of this antagonist, we selected two different doses (18.75 and 37.5 mg/Kg UBP141; Fig.5B) based on the work by Lozovaya and colleagues (Lozovava et al., 2014). AIMs were evaluated before (day −1) and after (day 0) UBP141 and last L-DOPA administration. Our results indicated that acute i.p. injection of 37.5 mg/Kg UBP141 was effective in ameliorating the dyskinetic motor behavior in our rat model of experimental LID (Fig.5B; $n = 4$; paired Student's t-test, 18.75 mg/Kg: $p > .05$, 37.5 mg/Kg: $p = .0479$). Once we determined the treatment conditions for acute UBP141 systemic administration, parkinsonian rats were chronically treated with L-DOPA for two weeks, and those with a solid dyskinetic behaviour underwent a single i.p. injection of 37.5 mg/Kg UBP141 or vehicle (saline) 30 min before the last L-DOPA administration. AIMs evaluation was carried out the day before UBP141 treatment and after the injection of the antagonist/vehicle. Our data showed that UBP141 reduced the dyskinetic behavior of treated animals (Fig.5C; $n = 8$; Two-way ANOVA followed by Bonferroni post-hoc analysis, $^*p < .05$ UBP141 day −1 vs UBP141 day 0, #p < .05 VEHICLE day 0 vs UBP141 day 0). Altogether these *in vivo* experiments support a role for GluN2D-containing NMDARs in LID.

4. Discussion

The glutamatergic signaling from the cortical afferents to the striatum undergoes adaptive changes after chronic treatment with L-DOPA leading to an aberrant release of glutamate together with an altered subunit composition and activity of NMDARs at SPN synapses (Mellone and Gardoni, 2013; Sgambato-Faure and Cenci, 2012). Our findings extend previous observations obtained in dopamine-depleted animals (Zhang and Chergui, 2015) and newly demonstrate a role for GluN2D-containing NMDARs in LID. Here we show that acute treatment, both intrastriatal and systemic, with a well-validated GluN2D subunit specific NMDAR antagonist (UBP141) significantly reduces the severity of established dyskinesia in L-DOPA-treated rats. In particular, we show that UBP141 delays the onset of the dyskinetic motor behaviour after L-DOPA challenge. Further studies are needed to evaluate the chronic therapeutic effect of GluN2D-specific antagonists in preventing LID.

We demonstrate that GluN2D subunit is significantly augmented at the striatal postsynaptic membranes of L-DOPA-treated dyskinetic rats. It is known that GluN2D-containing receptors are exclusively expressed by striatal ChIs in physiological conditions (Bloomfield et al., 2007; Zhang and Chergui, 2015; Tozzi et al., 2016). Our immunohistochemistry and electrophysiology experiments confirm the absence of GluN2D subunit in SPNs of control rats, while they clearly demonstrate its appearance in SPNs of dyskinetic animals. Only a trend towards an increase of GluN2D-NMDARs at synapses was observed both

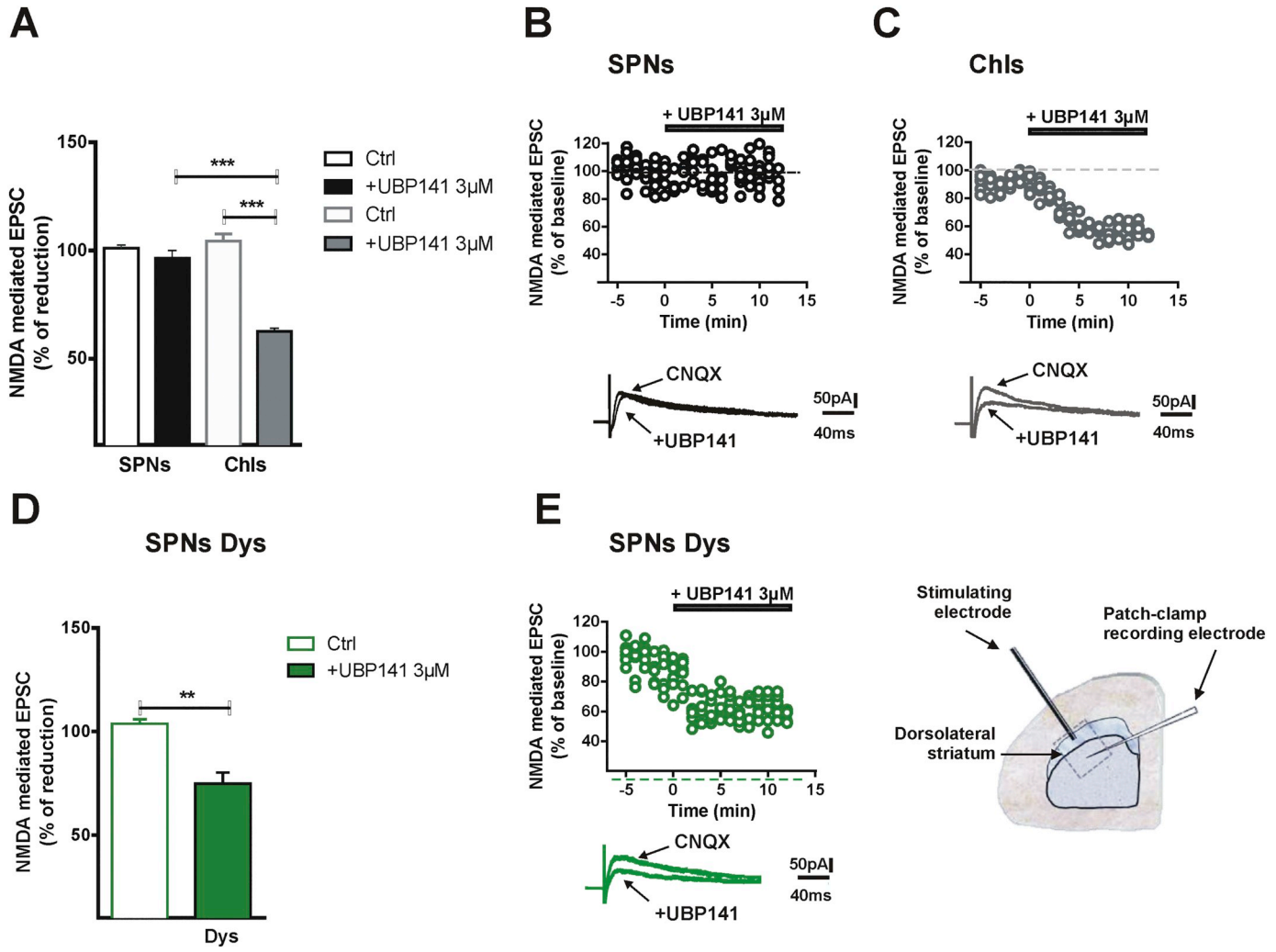

Fig. 4. Electrophysiological measurements of UBP141 distinct effects of striatal neuronal subtypes in control and dyskinetic rats. (A) Histogram showing the reduction of the NMDA receptor-mediated EPSC amplitude of SPNs (n = 6) and ChIs (n = 5) after 15 min of UBP141 application with respect to predrug conditions (50 μmol/L Picrotoxin plus 10 μmol/L CNQX) (UBP141 in SPNs versus ChIs, $t = 7.317$, dt = 10, $^{***}p \geq .001$). Reduction of EPSC amplitude of ChIs compared to SPNs (paired Student *t*-test, $t = 9.025$, df = 4, $^{***}p \leq .001$). Time course and representative EPSC traces (insets) of the NMDA receptor-mediated EPSC amplitude recorded from a single SPN (B) and a ChI (C) before and during the application of 3 μmol/L UBP141. (D) Histogram showing the reduction of the NMDA receptor-mediated EPSC amplitude of SPNs recorded from dyskinetic rats (n = 5, Student t-test, $t = 6.124$, dt = 4, $^{**}p \leq .01$) after 15 min of UBP141 application with respect to predrug conditions (50 μmol/L Picrotoxin plus 10 μmol/L CNQX). (E) Time course and representative EPSC traces (insets) of the NMDA receptor-mediated EPSC amplitude recorded from a single SPN of dyskinetic 6-OHDA-injected rats before and during the application of 3 μmol/L UBP141 (left panel). Representative electrophysiological electrodes positioning in the dorsolateral striatum (right panel).

in parkinsonian and dyskinetic monkeys. However, this apparent discrepancy can be ascribed to different reasons, including i. a mild postsynaptic purification protocol used for the monkey tissue, ii. the use of two different genders, male 6-OHDA lesioned rats and female MPTP-monkeys, and iii. a limited number of monkeys used in the present work. Additional studies are required for a more careful analysis of GluN2D expression in SPNs vs. ChIs in the monkey model as well as a further validation in post-mortem tissue from PD patients.

Protein-protein interactions at the C-terminal domain of NMDAR GluN2 subunits control the receptor subcellular localization and binding to specific signaling molecules. Members of the PSD-MAGUK family of scaffolding proteins, such as PSD-95, participate to the molecular organization of NMDARs at the postsynaptic density and regulate interactions between these receptors and their downstream signaling effectors (Chen et al., 2015; Cousins et al., 2008; Frank and Grant, 2017). Previous studies from our groups demonstrated changes in the association of GluN2A- and GluN2B-expressing NMDARs to proteins of the PSD-MAGUK family at SPN synapses (Gardoni et al., 2006; Mellone et al., 2015). In particular, disruption of GluN2A/PSD-95 binding improves the abnormal motor phenotype of dyskinetic rats and monkeys (Gardoni et al., 2012; Mellone et al., 2015; Stanic et al., 2017), indicating that aberrant protein-protein associations are involved in the adaptive mechanisms following DA depletion and chronic L-DOPA administration. Conversely, only scattered information is available about the physiological role of GluN2D interaction with scaffolding proteins and its possible role in central nervous system disorders (Cousins et al., 2008; Tozzi et al., 2016). We recently reported that, in the striatum, GluN2D-containing NMDARs are enriched in the postsynaptic densities where they interact with PSD-95 (Tozzi et al., 2016). Here we show that increased levels of synaptic GluN2D-containing NMDARs in dyskinetic rats are linked to changes in the receptor binding to PSD-95. Interestingly, this event is also correlated to a trend towards a decreased interaction with GluN2D to the guanine nucleotide exchange factor Dock3, which has been reported to reduce the surface expression of this NMDAR subtype (Bai et al., 2013). Accordingly, our work is in line with previous reports on PD and LID which describe abnormalities in NMDAR subcellular distribution and interaction with protein partners (Mellone and Gardoni, 2013; Sgambato-Faure and Cenci, 2012).

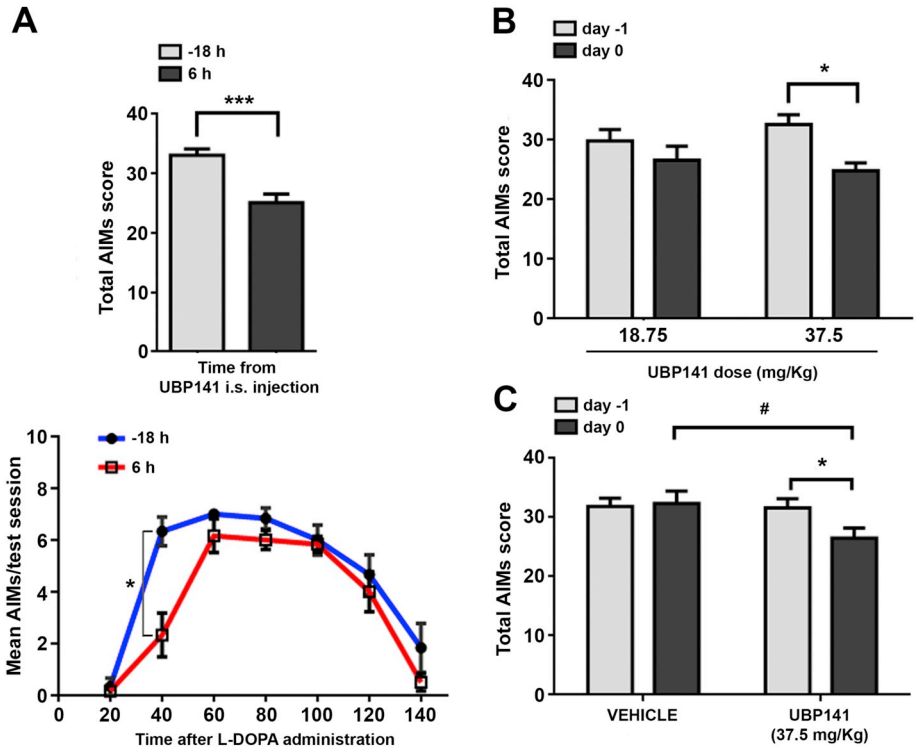

Fig. 5. Effect of in vivo modulation of GluN2D-expressing NMDARs in parkinsonian rats displaying a dyskinetic motor behavior. (A) AIMs were evaluated the day before (−18 h) and 6 h after the intrastriatal (i.s.) injection of 5 nmol UBP141, a GluN2D NMDAR antagonist, in the ipsilateral striatum of 6-OHDA rats chronically treated with L-DOPA and presenting a dyskinetic behavior - Total AIMs score (*top panel*): n = 6, ***p < .001, paired Student's t-test; mean AIMs per test session indicating AIMs induction: *p < .05 40 min −18 h vs 6 h, paired Student's t-test. (B) Two different doses of UBP141 (18.75 and 37.5 mg/Kg) were administrated systemically (i.p.) to dyskinetic rats 30 min before the last L-DOPA injection. AIMs were evaluated the day before (day −1) and after UBP141 administration (day 0) - 37.5 mg/Kg: $n = 4$, *p < .05, paired Student's t-test. (C) Acute i.p. injection of either UBP141 (37.5 mg/Kg) or vehicle (saline). Two-way ANOVA followed by Bonferroni post-hoc analysis, $n = 8$, *p < .05 UBP141 day-1 vs UBP141 day 0, #p < .05 UBP141 day 0 vs vehicle day 0.

Finally, the present study confirms the central role of PSD-95-mediated interactions at striatal SPN synapses in LID onset. In fact, previous papers indicated that an aberrant PSD-95 subcellular distribution (Nash et al., 2005; Porras et al., 2012) as well as an excessive interaction not only with NMDAR subunits but also with D1-type DA receptors are strictly correlated to LID (Porras et al., 2012).

GluN2D-NMDAR expression is restricted to few regions of the adult brain and few cell types compared to other main and widely expressed NMDAR regulatory subunits, namely GluN2A and GluN2B (Dunah et al., 1996, 1998; Monyer et al., 1994; Wenzel et al., 1996). This represents a major advantage from a therapeutic point of view as inhibition of GluN2D-containing NMDARs to counteract dyskinesia can be more selective and less associated to the onset of side effects compared to compounds targeting GluN2A and GluN2B-NMDARs. Furthermore, while GluN2A and GluN2B subunits intracellular C-tail are similar, that of GluN2D is shorter and its structure strongly differs from the former two. This provides a further degree of selectivity when thinking of a therapeutic strategy targeting GluN2D/PSD-95 complexes.

In summary, here we confirm and expand the emerging concept that cell-type and subunit specific modifications of NMDARs in the striatum underlie the pathophysiology of PD and LID. In physiological conditions, while GluN2B is present in both SPNs and ChIs, GluN2A is expressed only in SPNs (Vastagh et al., 2012) and GluN2D-containing receptors are exclusively found in striatal ChIs (Bloomfield et al., 2007; Zheng and Chergui, 2015; Tozzi et al., 2016). Considering that LIDs are characterized at SPN by i. a previously reported increased synaptic localization of GluN2A (Gardoni et al., 2006, 2012; Mellone et al., 2015), ii. a redistribution of GluN2B-expressing subtypes to the extrasynaptic membrane (Gardoni et al., 2006) and iii. an increased levels of synaptic GluN2D-NMDARs at SPN synapses here reported, our data support the existence of a complex pattern of modifications of NMDAR at the corticostriatal glutamatergic synapse that can be targeted with subunit-specific antagonists or peptides interfering with subunit-specific interactions with scaffolding proteins.

Conflict of interest

EB has an equity stake in Motac holding Ltd. and receives consultancy payments from Motac Neuroscience Ltd.

Funding

This work was supported by Min. San. RF-2013-02356215, Cariplo Foundation project 2014-0660 and PRIN2015FNWP34 to FG and to PC; Fondazione Umberto Veronesi Fellowship – Grants 2015 to MM. Current grant support to EB includes Agence Nationale de la Recherche, China Science Fund, Michael J Fox Foundation for Parkinson Research, France Parkinson, Fondation de France, Medical Research Council, Innovative Medicines Initiative, European Commission (H2020, IMPRIND), IDEX Bordeaux, COEN, MSA Coalition, Rotary Foundation, Nouvelle-Aquitaine Regional Council, and LABEX Brain.

Acknowledgements

The authors are thankful to Elisa Montanari, Sabrina Nuzzo and Francesca Rusconi for their technical support.

References

Ahmed, M.R., Berthet, A., Bychkov, E., Porras, G., Li, Q., Bioulac, B.H., Carl, Y.T., Bloch, B., Kook, S., Aubert, I., Dovero, S., Doudnikoff, E., Gurevich, V.V., Gurevich, E.V., Bezard, E., 2010. Lentiviral overexpression of GRK6 alleviates L-dopa-induced dyskinesia in experimental Parkinson's disease. Sci. Transl. Med. 2, 28ra28.

Bai, N., Hayashi, H., Aida, T., Namekata, K., Harada, T., Mishina, M., Tanaka, K., 2013. Dock3 interaction with a glutamate-receptor NR2D subunit protects neurons from excitotoxicity. Mol. Brain 4, 22.

Bastide, M.F., Meissner, W.G., Picconi, B., Fasano, S., Fernagut, P.O., Feyder, M., Francardo, V., Alcacer, C., Ding, Y., Brambilla, R., Fisone, G., Jon Stoessl, A., Bourdenx, M., Engeln, M., Navailles, S., De Deurwaerdère, P., Ko, W.K., Simola, N., Morelli, M., Groc, L., Rodriguez, M.C., Gurevich, E.V., Quik, M., Morari, M., Mellone, M., Gardoni, F., Tronci, E., Guehl, D., Tison, F., Crossman, A.R., Kang, U.J., Steece-Collier, K., Fox, S., Carta, M., Angela Cenci, M., Bézard, E., 2015. Pathophysiology of L-dopa-induced motor and non-motor complications in Parkinson's disease. Prog. Neurobiol. 132, 96–168.

Bloomfield, C., O'Donnell, P., French, S.J., Totterdell, S., 2007. Cholinergic neurons of the adult rat striatum are immunoreactive for glutamatergic N-methyl-d-aspartate 2D but

not N-methyl-d-aspartate 2C receptor subunits. Neuroscience 150, 639–646.
Bonsi, P., Cuomo, D., Martella, G., Madeo, G., Schirinzi, T., Puglisi, F., Ponterio, G., Pisani, A., 2011. Centrality of striatal cholinergic transmission in Basal Ganglia function. Front. Neuroanat. 5 (6).
Bourdenx, M., Dovero, S., Engeln, M., Bido, S., Bastide, M.F., Dutheil, N., Vollenweider, I., Baud, L., Piron, C., Grouthier, V., Boraud, T., Porras, G., Li, Q., Baekelandt, V., Scheller, D., Michel, A., Fernagut, P.O., Georges, F., Courtine, G., Bezard, E., Dehay, B., 2015. Lack of additive role of ageing in nigrostriatal neurodegeneration triggered by α-synuclein overexpression. Acta Neuropathol. Commun 25, 46.
Calabresi, P., Picconi, B., Tozzi, A., Di Filippo, M., 2007. Dopamine-mediated regulation of corticostriatal synaptic plasticity. Trends Neurosci. 30, 211–219.
Calabresi, P., Picconi, B., Tozzi, A., Ghiglieri, V., Di Filippo, M., 2014. Direct and indirect pathways of basal ganglia: a critical reappraisal. Nat. Neurosci. 17, 1022–1030.
Cenci, M.A., Lundblad, M., 2007. Ratings of L-DOPA-induced dyskinesia in the unilateral 6-OHDA lesion model of Parkinson's disease in rats and mice. Curr. Protoc. Neurosci. Chapter 9, Unit 9, 25.
Centonze, D., Gubellini, P., Bernardi, G., Calabresi, P., 1999. Permissive role of interneurons in corticostriatal synaptic plasticity. Brain Res. Brain Res. Rev. 31, 1–5.
Chen, X., Levy, J.M., Hou, A., Winters, C., Azzam, R., Sousa, A.A., Leapman, R.D., Nicoll, R.A., Reese, T.S., 2015. PSD-95 family MAGUKs are essential for anchoring AMPA and NMDA receptor complexes at the postsynaptic density. Proc. Natl. Acad. Sci. U. S. A. 112, E6983–E6992.
Connolly, B.S., Lang, A.E., 2014. Pharmacological treatment of Parkinson disease: a review. JAMA 311, 1670–1683.
Costa, A., Peppe, A., Dell'Agnello, G., Caltagirone, C., Carlesimo, G.A., 2009. Dopamine and cognitive functioning in de novo subjects with Parkinson's disease: effects of pramipexole and pergolide on working memory. Neuropsychologia 47, 1374–1381.
Cousins, S.L., Papadakis, M., Rutter, A.R., Stephenson, F.A., 2008. Differential interaction of NMDA receptor subtypes with the post-synaptic density-95 family of membrane associated guanylate kinase proteins. J. Neurochem. 104, 903–913.
Da Silva-Júnior, F.P., Braga-Neto, P., Sueli Monte, F., de Bruin, V.M., 2005. Amantadine reduces the duration of levodopa-induced dyskinesia: a randomized, double-blind, placebo-controlled study. Parkinsonism Relat. Disord. 11, 449–452.
Davies, S.E., Hallett, P.J., Moens, T., Smith, G., Mangano, E., Kim, H.T., Goldberg, A.L., Liu, J.L., Isacson, O., Tofaris, G.K., 2014. Enhanced ubiquitin-dependent degradation by Nedd4 protects against α-synuclein accumulation and toxicity in animal models of Parkinson's disease. Neurobiol. Dis. 64, 79–87.
Dunah, A.W., Yasuda, R.P., Wang, Y.H., Luo, J., Dávila-García, M., Gbadegesin, M., Vicini, S., Wolfe, B.B., 1996. Regional and ontogenic expression of the NMDA receptor subunit NR2D protein in rat brain using a subunit-specific antibody. J. Neurochem. 67, 2335–2345.
Dunah, A.W., Luo, J., Wang, Y.H., Yasuda, R.P., Wolfe, B.B., 1998. Subunit composition of N-methyl-D-aspartate receptors in the central nervous system that contain the NR2D subunit. Mol. Pharmacol. 53, 429–437.
Elahi, B., Phielipp, N., Chen, R., 2012. N-Methyl-D-Aspartate antagonists in levodopa induced dyskinesia: a meta-analysis. Can. J. Neurol. Sci. 39, 465–472.
English, D.F., Ibanez-Sandoval, O., Stark, E., Tecuapetla, F., Buzsáki, G., Deisseroth, K., Tepper, J.M., Koos, T., 2011. GABAergic circuits mediate the reinforcement-related signals of striatal cholinergic interneurons. Nat. Neurosci. 15, 123–130.
Feng, Z.J., Zhang, X., Chergui, K., 2014. Allosteric modulation of NMDA receptors alters neurotransmission in the striatum of a mouse model of Parkinson's disease. Exp. Neurol. 255, 154–160.
Fernagut, P.O., Li, Q., Dovero, S., Chan, P., Wu, T., Ravenscroft, P., Hill, M., Chen, Z., Bezard, E., 2010. Dopamine transporter binding is unaffected by L-DOPA administration in normal and MPTP-treated monkeys. PLoS One 5, e14053.
Frank, R.A., Grant, S.G., 2017. Supramolecular organization of NMDA receptors and the postsynaptic density. Curr. Opin. Neurobiol. 45, 139–147.
Gardoni, F., Di Luca, M., 2015. Targeting glutamatergic synapses in Parkinson's disease. Curr. Opin. Pharmacol. 20, 24–28.
Gardoni, F., Picconi, B., Ghiglieri, V., Polli, F., Bagetta, V., Bernardi, G., Cattabeni, F., Di Luca, M., Calabresi, P., 2006. A critical interaction between NR2B and MAGUK in L-DOPA induced dyskinesia. J. Neurosci. 26, 2914–2922.
Gardoni, F., Sgobio, C., Pendolino, V., Calabresi, P., Di Luca, M., Picconi, B., 2012. Targeting NR2A-containing NMDA receptors reduces L-DOPA-induced dyskinesias. Neurobiol. Aging 33, 2138–2144.
Gautam, V., Trinidad, J.C., Rimerman, R.A., Costa, B.M., Burlingame, A.L., Monaghan, D.T., 2013. Nedd4 is a specific E3 ubiquitin ligase for the NMDA receptor subunit GluN2D. Neuropharmacology 74, 96–107.
Ghiglieri, V., Mineo, D., Vannelli, A., Cacace, F., Mancini, M., Pendolino, V., Napolitano, F., di Maio, A., Mellone, M., Stanic, J., Tronci, E., Fidalgo, C., Stancampiano, R., Carta, M., Calabresi, P., Gardoni, F., Usiello, A., Picconi, B., 2015. Modulation of serotonergic transmission by eltoprazine in L-DOPA-induced dyskinesia: Behavioral, molecular, and synaptic mechanisms. Neurobiol. Dis. 86, 140–153.
Glasgow, N.G., Siegler Retchless, B., Johnson, J.W., 2015. Molecular bases of NMDA receptor subtype-dependent properties. J. Physiol. 593, 83–95.
Goedert, M., Jakes, R., Spillantini, M.G., 2017. The Synucleinopathies: Twenty Years On. J. Parkinsons. Dis. 7, S53–S71.
Goldberg, J.A., Ding, J.B., Surmeier, D.J., 2012. Muscarinic modulation of striatal function and circuitry. Handb. Exp. Pharmacol. 208, 223–241.
Jones, S., Gibb, A.J., 2005. Functional NR2B- and NR2D-containing NMDA receptor channels in rat substantia nigra dopaminergic neurones. J. Physiol. 569, 209–221.
Kaneko, S., Hikida, T., Watanabe, D., Ichinose, H., Nagatsu, T., Kreitman, R.J., Pastan, I., Nakanishi, S., 2000. Synaptic integration mediated by striatal cholinergic interneurons in basal ganglia function. Science 289, 633–637.
Landwehrmeyer, G.B., Standaert, D.G., Testa, C.M., Penney, J.B. Jr, Young, A.B., 1995. NMDA receptor subunit mRNA expression by projection neurons and interneurons in rat striatum. J. Neurosci. 15, 5297–5307.
Lozovaya, N., Gataullina, S., Tsintsadze, T., Tsintsadze, V., Pallesi-Pocachard, E., Minlebaev, M., Goriounova, N.A., Buhler, E., Watrin, F., Shityakov, S., Becker, A.J., Bordey, A., Milh, M., Scavarda, D., Bulteau, C., Dorfmuller, G., Delalande, O., Represa, A., Cardoso, C., Dulac, O., Ben-Ari, Y., Burnashev, N., 2014. Selective suppression of excessive GluN2C expression rescues early epilepsy in a tuberous sclerosis murine model. Nat. Commun. 5, 4563.
Lundblad, M., Andersson, M., Winkler, C., Kirik, D., Wierup, N., Cenci, M.A., 2002. Pharmacological validation of behavioural measures of akinesia and dyskinesia in a rat model of Parkinson's disease. Eur. J. Neurosci. 15, 120–132.
Mellone, M., Gardoni, F., 2013. Modulation of NMDA receptor at the synapse: promising therapeutic interventions in disorders of the nervous system. Eur. J. Pharmacol. 719, 75–83.
Mellone, M., Gardoni, F., 2018. Glutamatergic mechanisms in L-DOPA-induced dyskinesia and therapeutic implications. J. Neural Transm. (Vienna) 125 (8), 1225–1236 (Aug).
Mellone, M., Stanic, J., Hernandez, L.F., Iglesias, E., Zianni, E., Longhi, A., Prigent, A., Picconi, B., Calabresi, P., Hirsch, E.C., Obeso, J.A., Di Luca, M., Gardoni, F., 2015. NMDA receptor GluN2A/GluN2B subunit ratio as synaptic trait of levodopa-induced dyskinesias: from experimental models to patients. Front. Cell. Neurosci. 9, 245.
Merello, M., Nouzeilles, M.I., Cammarota, A., Leiguarda, R., 1999. Effect of memantine (NMDA antagonist) on Parkinson's disease: a double-blind crossover randomized study. Clin. Neuropharmacol. 22, 273–276.
Monyer, H., Burnashev, N., Laurie, D.J., Sakmann, B., Seeburg, P.H., 1994. Developmental and regional expression in the rat brain and functional properties of four NMDA receptors. Neuron 12, 529–540.
Moreau, C., Delval, A., Tiffreau, V., Defebvre, L., Dujardin, K., Duhamel, A., Petyt, G., Hossein-Foucher, C., Blum, D., Sablonnière, B., Schraen, S., Allorge, D., Destée, A., Bordet, R., Devos, D., 2013. Memantine for axial signs in Parkinson's disease: a randomised, double-blind, placebo-controlled pilot study. J. Neurol. Neurosurg. Psychiatry 84, 552–555.
Morley, R.M., Tse, H.W., Feng, B., Miller, J.C., Monaghan, D.T., Jane, D.E., 2005. Synthesis and pharmacology of N1-substituted piperazine-2,3-dicarboxylic acid derivatives acting as NMDA receptor antagonists. J. Med. Chem. 48, 2627–2637.
Nash, J.E., Johnston, T.H., Collingridge, G.L., Garner, C.C., Brotchie, J.M., 2005. Subcellular redistribution of the synapse-associated proteins PSD-95 and SAP97 in animal models of Parkinson's disease and L-DOPA-induced dyskinesia. FASEB J. 19, 583–585.
Ory-Magne, F., Corvol, J.C., Azulay, J.P., Bonnet, A.M., Brefel-Courbon, C., Damier, P., Dellapina, E., Destée, A., Durif, F., Galitzky, M., Lebouvier, T., Meissner, W., Thalamas, C., Tison, F., Salis, A., Sommet, A., Viallet, F., Vidailhet, M., Rascol, O., Network, NS-Park C.I.C., 2014. Withdrawing amantadine in dyskinetic patients with Parkinson disease: the AMANDYSK trial. Neurology 82, 300–307.
Paillé, V., Picconi, B., Bagetta, V., Ghiglieri, V., Sgobio, C., Filippo, M., Viscomi, M.T., Giampà, C., Fusco, F.R., Gardoni, F., Bernardi, G., Greengard, P., Luca, M., Calabresi, P., 2010. Distinct levels of dopamine denervation differentially alter striatal synaptic plasticity and NMDA receptor subunit composition. J. Neurosci. 30 (42), 14182–14193 (Oct 20).
Pakhotin, P., Bracci, E., 2007. Cholinergic interneurons control the excitatory input to the striatum. J. Neurosci. 27, 391–400.
Paoletti, P., Bellone, C., Zhou, Q., 2013. NMDA receptor subunit diversity: impact on receptor properties, synaptic plasticity and disease. Nat. Rev. Neurosci. 14, 383–400.
Perez, X.A., Bordia, T., Quik, M., 2018. The striatal cholinergic system in L-dopa-induced dyskinesias. J. Neural Transm. (Vienna) 125, 1251–1262.
Perszyk, R.E., Diraddo, J.O., Strong, K.L., Low, C.M., Ogden, K.K., Khatri, A., Vargish, G.A., Pelkey, K.A., Tricoire, L., Liotta, D.C., Smith, Y., McBain, C.J., Traynelis, S.F., 2016. GluN2D-Containing N-methyl-d-Aspartate Receptors Mediate Synaptic Transmission in Hippocampal Interneurons and Regulate Interneuron Activity. Mol. Pharmacol. 90, 689–702.
Picconi, B., Centonze, D., Håkansson, K., Bernardi, G., Greengard, P., Fisone, G., Cenci, M.A., Calabresi, P., 2003. Loss of bidirectional striatal synaptic plasticity in L-DOPA-induced dyskinesia. Nat. Neurosci. 6, 501–506.
Picconi, B., De Leonibus, E., Calabresi, P., 2018. Synaptic plasticity and levodopa-induced dyskinesia: electrophysiological and structural abnormalities. J. Neural Transm. (Vienna) 125 (8), 1263–1271 (Aug).
Pisani, A., Bernardi, G., Ding, J., Surmeier, D.J., 2007. Re-emergence of striatal cholinergic interneurons in movement disorders. Trends Neurosci. 30, 545–553.
Porras, G., Berthet, A., Dehay, B., Li, Q., Ladepeche, L., Normand, E., Dovero, S., Martinez, A., Doudnikoff, E., Martin-Négrier, M.L., Chuan, Q., Bloch, B., Choquet, D., Boué-Grabot, E., Groc, L., Bezard, E., 2012. PSD-95 expression controls L-DOPA dyskinesia through dopamine D1 receptor trafficking. J. Clin. Invest. 122, 3977–3989.
Rotin, D., Kumar, S., 2009. Physiological functions of the HECT family of ubiquitin ligases. Nat. Rev. Mol. Cell Biol. 10, 398–409.
Santini, E., Sgambato-Faure, V., Li, Q., Savasta, M., Dovero, S., Fisone, G., Bezard, E., 2010. Distinct changes in cAMP and extracellular signal-regulated protein kinase signalling in L-DOPA-induced dyskinesia. PLoS One 5, e12322.
Sgambato-Faure, V., Cenci, M.A., 2012. Glutamatergic mechanisms in the dyskinesias induced by pharmacological dopamine replacement and deep brain stimulation for the treatment of Parkinson's disease. Prog. Neurobiol. 96, 69–86.
Standaert, D.G., Testa, C.M., Young, A.B., Penney Jr., J.B., 1994. Organization of N-methyl-D-aspartate glutamate receptor gene expression in the basal ganglia of the rat. J. Comp. Neurol. 343, 1–16.
Stanic, J., Mellone, M., Cirnaru, M.D., Perez-Carrion, M., Zianni, E., Di Luca, M., Gardoni, F., Piccoli, G., 2016. LRRK2 phosphorylation level correlates with abnormal motor behaviour in an experimental model of levodopa-induced dyskinesias. Mol Brain 11 9

(1), 53.
Stanic, J., Mellone, M., Napolitano, F., Racca, C., Zianni, E., Minocci, D., Ghiglieri, V., Thiolat, M.L., Li, Q., Longhi, A., De Rosa, A., Picconi, B., Bezard, E., Calabresi, P., Di Luca, M., Usiello, A., Gardoni, F., 2017. Rabphilin 3A: A novel target for the treatment of levodopa-induced dyskinesias. Neurobiol. Dis. 108, 54–64.
Suárez, F., Zhao, Q., Monaghan, D.T., Jane, D.E., Jones, S., Gibb, A.J., 2010. Functional heterogeneity of NMDA receptors in rat substantia nigra pars compacta and reticulata neurones. Eur. J. Neurosci. 32, 359–367.
Swanger, S.A., Vance, K.M., Pare, J.F., Sotty, F., Fog, K., Smith, Y., Traynelis, S.F., 2015. NMDA Receptors Containing the GluN2D Subunit Control Neuronal Function in the Subthalamic Nucleus. J. Neurosci. 35, 15971–15983.
Threlfell, S., Lalic, T., Platt, N.J., Jennings, K.A., Deisseroth, K., Cragg, S.J., 2012. Striatal dopamine release is triggered by synchronized activity in cholinergic interneurons. Neuron 75, 58–64.
Tofaris, G.K., Kim, H.T., Hourez, R., Jung, J.W., Kim, K.P., Goldberg, A.L., 2011. Ubiquitin ligase Nedd4 promotes alpha-synuclein degradation by the endosomal-lysosomal pathway. Proc. Natl. Acad. Sci. U. S. A. 108, 17004–17009.
Tozzi, A., de Iure, A., Bagetta, V., Tantucci, M., Durante, V., Quiroga-Varela, A., Costa, C., Di Filippo, M., Ghiglieri, V., Latagliata, E.C., Wegrzynowicz, M., Decressac, M., Giampà, C., Dalley, J.W., Xia, J., Gardoni, F., Mellone, M., El-Agnaf, O.M., Ardah, M.T., Puglisi-Allegra, S., Björklund, A., Spillantini, M.G., Picconi, B., Calabresi, P., 2016. Alpha-Synuclein Produces Early Behavioral Alterations via Striatal Cholinergic Synaptic Dysfunction by Interacting With GluN2D N-Methyl-D-Aspartate Receptor Subunit. Biol. Psychiatry 79, 402–414.
Traynelis, S.F., Wollmuth, L.P., McBain, C.J., Menniti, F.S., Vance, K.M., Ogden, K.K., Hansen, K.B., Yuan, H., Myers, S.J., Dingledine, R., 2010. Glutamate receptor ion channels: structure, regulation, and function. Pharmacol. Rev. 62, 405–496.
Tronci, E., Fidalgo, C., Zianni, E., Collu, M., Stancampiano, R., Morelli, M., Gardoni, F., Carta, M., 2014. Effect of memantine on L-DOPA-induced dyskinesia in the 6-OHDA-lesioned rat model of Parkinson's disease. Neuroscience 18 (265), 245–252.
Urs, N.M., Bido, S., Peterson, S.M., Daigle, T.L., Bass, C.E., Gainetdinov, R.R., Bezard, E., Caron, M.G., 2015. Targeting β-arrestin2 in the treatment of L-DOPA-induced dyskinesia in Parkinson's disease. Proc. Natl. Acad. Sci. U. S. A. 112, E2517–E2526.
Varanese, S., Howard, J., Di Rocco, A., 2010. NMDA antagonist memantine improves levodopa-induced dyskinesias and "on-off" phenomena in Parkinson's disease. Mov. Disord. 25, 508–510.
Vastagh, C., Gardoni, F., Bagetta, V., Stanic, J., Zianni, E., Giampà, C., Picconi, B., Calabresi, P., Di Luca, M., 2012. N-methyl-D-aspartate (NMDA) receptor composition modulates dendritic spine morphology in striatal medium spiny neurons. J. Biol. Chem. 287, 18103–18114.
Vicini, S., Wang, J.F., Li, J.H., Zhu, W.J., Wang, Y.H., Luo, J.H., Wolfe, B.B., Grayson, D.R., 1998. Functional and pharmacological differences between recombinant N-methyl-D-aspartate receptors. J. Neurophysiol. 79, 555–566.
Wenzel, A., Villa, M., Mohler, H., Benke, D., 1996. Developmental and regional expression of NMDA receptor subtypes containing the NR2D subunit in rat brain. J. Neurochem. 66, 1240–1248.
Wolf, E., Seppi, K., Katzenschlager, R., Hochschorner, G., Ransmayr, G., Schwingenschuh, P., Ott, E., Kloiber, I., Haubenberger, D., Auff, E., Poewe, W., 2010. Long-term antidyskinetic efficacy of amantadine in Parkinson's disease. Mov. Disord. 25, 1357–1363.
Yamamoto, H., Kamegaya, E., Sawada, W., Hasegawa, R., Yamamoto, T., Hagino, Y., Takamatsu, Y., Imai, K., Koga, H., Mishina, M., Ikeda, K., 2013. Involvement of the N-methyl-D-aspartate receptor GluN2D subunit in phencyclidine-induced motor impairment, gene expression, and increased Fos immunoreactivity. Mol. Brain 16, 56.
Zhang and Chergui, 2015. Dopamine depletion of the striatum causes a cell-type specific reorganization of GluN2B- and GluN2D-containing NMDA receptors. Neuropharmacology 92, 108–115.
Zhang, X., Feng, Z.J., Chergui, K., 2014. GluN2D-containing NMDA receptors inhibit neurotransmission in the mouse striatum through a cholinergic mechanism: implication for Parkinson's disease. J. Neurochem. 129, 581–590.